SCIREA Journal of Electrical Engineering

http://www.scirea.org/journal/DEE

May 10, 2020

Volume 5, Issue 2, April 2020

Automatic Hair Colorization and Relighting Using Chromaticity Distribution Matching

Uri Lipowezky

Research and Development Department/Facetrom, Tel Aviv, Israel

Email: urilip@aim.com

Abstract

Human hair colorization, concerning given model hair image without changing neither hairstyle nor hair texture, is a challenging task. The principle problem making this task complicated is the difference in the texture and the illumination between a user and model images. The natural human hair consists of a mix of hair swatches. Each swatch has its chromaticity distribution, which, generally, is non-Gaussian. These swatches can be determined as color clusters in the hair image. In this case, the problem can be solved by matching between the user and the model hair swatches or color clusters. After this matching, the color transfer between the relevant model and user swatches is applied. Besides, the model's hair should be compressed to a reasonable size to provide simultaneous representation for a variety of hair colors. The model's hair colors are taken from the images of hair color packs usually available in decorative cosmetic stores. These images, however, are taken in standard illumination condition, so appropriate relighting should be applied to provide photorealistic user's image. Experimental results with 530 different color models, and more than 20,000 users show that the proposed technique achieves high photorealistic

perception and a reasonable compression ratio.

Keywords: Color measurement, Image color analysis, Chromaticity distribution, Probability distributions matching

1. Introduction

The automatic human hair colorization task is motivated by the hair color marketing incentive. Hair color products cannot be easily applied to the user's hair, and for a user, it is difficult to decide which of the model hair colors that are shown up in the hair color pack, fits best to the user's hair. One of the possible techniques alleviating the user choice is hair color modeling available via the user photo uploading to the WEB sites [16], [17], or via automatic kiosk, e.g. [16]. Precise color transferring from the model to the user hair photo is a challenging problem due to the different hairstyles, hair textures, and illumination sources. Besides, the model's hair color description length is limited because it should be transferred online to the client site. As well, hair colorization should be applied fully automatically online, so Photoshop-based interactive methods like [18], which are widely used for advertising, cannot be used in real-life marketing.

Automatic hair recoloring technique supposes as an input a fuzzy user hair mask $\alpha(x,y)\epsilon[0,1]$, where (x,y) are the spatial coordinates of the user image and hair mask $\alpha = 0$ outside the hair area and $\alpha = 1$ inside the hair area. Fuzziness $0 < \alpha < 1$ is a powerful tool, allows overcoming uncertainness around hair roots, separate thin swatches, and margins. This mask can be painted either manually [18] or using user-assisted scribbles [7] or filly automatically [15], [9]. An example of a fully automatically created fuzzy hair mask [9], superimposed in the user photo, is displayed in Figure 1b.

(a) (b) (c) (d)

Figure 1. The original user's photo (a), fuzzy user hair mask (b), L'Oreal Paris Excellence 654 model photo (c), along with a superimposed manually painted hair mask, the user's photo after hair recoloring (d).

The existing solutions for image recoloring could be subdivided into user-assisted recoloring techniques and automatic recoloring techniques. User-assisted methods suppose an interactive color component transfer using the Photoshop hair colorization tool [18] in *HSV* color space, or using the color transfer brush tool [10]. The latter method is based on the local Gaussian distribution transfer (GDF) in the decorrelated color space $l\alpha\beta$ independently for each color component. Initially, this method was suggested by E. Reinhard et al. [12] in 2001. In the user image I_u, the transferred color at the pixel C_u is calculated as:

$$g(C_u) = \mu_m + \sigma_m\,(C_u - \mu_m)/\sigma_u, \qquad (1)$$

where μ_m, μ_u are the averages of the underlying user's and model's Gaussian distribution (cf. images Figure 1a and 1c). The values σ_u, σ_m are the standard deviations of the user and model Gaussian distributions.

Typically, there are three challenging problems in automatic recoloring for all kinds of natural images [4]: natural color image segmentation, image region mapping, and color transferring. The segmentation is applied to separate the whole picture into color support areas or superpixels [8] for further matching between the user's and the model's segments. Pyramidal edge merging [2] or Expectation-Maximization (EM) techniques [13], [14], accomplished with K-Mean [14] or Mean-Shift [2] clustering are power tools for the color image segmentation. Deep convolutional network SegNet [1], based on the VGG-16 encoder-decoder, can also be used for hair image segmentation.

The superpixels of the model's hair create a set of classes. Every user's hair superpixel has a chromaticity distribution. We can define a fitness function between this distribution and the model's superpixel, using, e.g., the Hotelling criterion. Thus, after an appropriate normalization, we have a fuzzy region mapping between the user's and the model's hair.

Besides the Hotelling test, a Gaussian Mixture Model (GMM) along with gentle boosting [13], [14] is another technique for this mapping. Eventually, GDF is used for local color transfer in $l\alpha\beta$ [14], HSV or YIQ [2] color spaces. These techniques provide photorealistic results for many natural images.

However, human hair images have five differences from typical natural scenes. First, the color distribution is not always Gaussian; second, $l\alpha\beta$ chrominance components have a high correlation ratio for human color. Some examples, given in table 1, show that the correlation ratio varies from 0.53 to 0.98 in a dataset of 530 human hair samples. That causes the GDF to produce false colors. Third, hair segments (swatches) are not separated one from another but smoothly transfer to each other. Besides, to provide a photo-realistic appearance, all hair swatches, mapped in the model, have to be reproduced in the user hair image. Thus, instead of the classification task, the matching between the superpixels of the user's and the model's images becomes a variation of the assignment problem [6].

Fourth, the entire model image is inaccessible for the end-user, but only a limited amount of color distribution parameters transferred online. Fifth, since only the hair is colorized independently from the rest parts of the facial image, generally speaking, the color could be unnatural because of the different illumination between the model and user images. So, the user image should be relighted by an appropriate white balance corrector to provide the photorealistic appearance.

This paper addresses the above issues, and it is proposed a method to transfer chrominance distribution (possible non-Gaussian) from the model to the user hair image. The proposed method is based on color lookup table (CLUT) usage in the different color spaces [2] along with the local chromaticity distribution transfer per each swatch with respect to GMM between the hair swatches. The process is accomplished with the white patch-based white rebalance [11] between the user's and the model's hairs.

Table 1. lαβ Chrominance correlation

Hair Color Number	Maximal $l\alpha\beta$ correlation ratio
200	0.6853
210	0.8368
300	0.8077
316	0.7145
400	0.8191
415	0.8852
426	0.6172
500	0.8849
565	0.7565
600	0.8271
643	0.8501
645	0.8024
656	0.5288
700	0.8752
713	0.9754
724	0.7955
810	0.9582
832	0.9762
834	0.7288
930	0.9711
Average	0.8148

2. Automatic Hair Color Transfer

Hair color transferring is processed in Yu^*v^* color space, where Y denotes the intensity component of $CIE\,YUV$ color space and u^*, v^* are the chromaticity components of the $CIELu^*v^*$ color space. The choosing of the $CIEYu^*v^*$ color space is motivated by its apparent reciprocal transformability into $CIE\,YSH$ color space [17]. Therefore, this color space also admits a smooth component-wise transfer for a specific swatch. The chromaticity is transformed into the hue and the saturation components as $S = \sqrt{(u^*)^2 + (v^*)^2}$ and $H = arctg(v^*/u^*)$. Figure 2 shows the graphic illustration of the YSH color space. Hair brightness Y is the most crucial component, affecting hair appearance. However, its typical distribution (see Figure 3d) is not similar to the Gaussian distribution, so the CLUT technique [7], [18], is adopted for component Y transfer and is denoted as YLUT. Let us denote D_m, m = 1...256 the cumulative histogram of the model and S_i is the user's cumulative histogram, i =1…256 (see Figure 3). Then, the direct YLUT is $L^d(i) = argmin(D_m \geq S_i)$ and the reverse is $L^r(i) = argmin(D_m \leq S_i)$. Since Y is a continuous variable and YLUT is a digital sampled value, the final transformed intensity is defined as follows:

$$y_t = \left[\tau\left(L^d\lceil y\rceil + L^r\lceil y\rceil\right) + (1-\tau)\left(L^d\lfloor y\rfloor + L^r\lfloor y\rfloor\right)\right]/2, \quad (2)$$

where $\tau = y - \lfloor y\rfloor$, symbol $\lfloor y\rfloor$ denotes the ceiling and $\lceil y\rceil$ the flooring functions. If the dynamic range of the user's photo is significantly low than the model's one, some bins are missing in the transformed histogram (see Figure 3). In this case, the Parzen-window estimator allows restoring the missed bins.

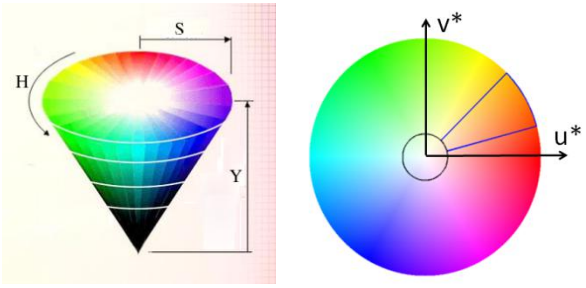

(a) (b)

Figure 2. YSH Color space (a) and hair swatch cluster (petal) in u^* v^* space (b).

2.1. Chromaticity Distribution Modeling

The YSH color space is modeled by the color cone (see Figure 2a). The cone vertex corresponds to the darkest hair swatch that is: $y_t \le Y_d$, where Y_d is the upper value below of which the color cannot be distinct by a customer; typically, $Y_d = 5$ for 256 bins transform. These swatches are less sensitive to the false-color injection and can be described by the correlated 2D Gaussian in the u^*v^* color space. The user's u^*v^* distribution is transformed into the model distribution using the 2D extension of Gaussian distribution function (GDF):

$$U'_t = U_t cos\alpha_m - V_t sin\alpha_m + \overline{U}_m \quad (3)$$

$$V'_t = U_t sin\alpha_m + V_t cos\alpha_m + \overline{V}_m. \quad (4)$$

In (3) and (4), $\overline{U}_m$ and $\overline{V}_m$ denotes the model averages. The rotation angle of the two-dimensional GDF is calculated as $\alpha = arctg\left[2\rho\sigma_u\sigma_v/\left(\sigma_u^2-\sigma_v^2\right)\right]/2$. Let us denote α_m the rotation angle for the model data and α_u for the user data. The distribution parameters σ_u and σ_v are the standard deviations and ρ is the Pearson correlation ratio between the chrominance components u^* and v^*. Values U_t and V_t are calculated as follows:

$$U_t = [(u-\overline{u})cos\alpha_u - (v-\overline{v})sin\alpha_u]\sqrt{\lambda_u^m/\lambda_u^u} \quad (5)$$

$$V_t = [(v-\overline{v})cos\alpha_u - (u-\overline{u})sin\alpha_u]\sqrt{\lambda_v^m/\lambda_v^u}, \quad (6)$$

where u and v are the user chromaticity for each pixel, $\overline{u}$ and $\overline{v}$ are the user averages, λ_u^m, λ_u^u, λ_v^m and λ_v^u are the eigenvalues for user and model u^*v^* distribution. These eigenvalues and are defined as follows:

$$\lambda_{u,v} = \left(\sigma_u^2+\sigma_v^2 \pm \sqrt{\left(\sigma_u^2-\sigma_v^2\right)^2+(2\rho\sigma_u\sigma_v)^2}\right)\Big/2. \quad (7)$$

The transformed user's chromaticity U_t, V_t has to be clipped into the $\left[U_{min}^m, U_{max}^m\right] \times \left[V_{min}^m, V_{max}^m\right]$ interval, consisting of the minimal and maximal values of the u^* and v^* components of the model's image, to prevent false colors appearance. Besides, to provide the correct color consistency, let us demand that transformed distribution should be spread over the 95% -quantile of the model distribution. The following limitation on the Mahalanobis distance is applied to supply this requirement [9].

$$\left(t_u^2+t_v^2-2t_u t_v\rho_m\right)/\left(1-\rho_m^2\right) \le -2ln(1-q), \quad (8)$$

where $t_u = (U_t - \overline{U}_m)/\sigma_u^m$, $t_v = (V_t - \overline{V}_m)/\sigma_v^m$ and ρ_m is the correlation ratio between the chrominance u^* and v^* on the model data.

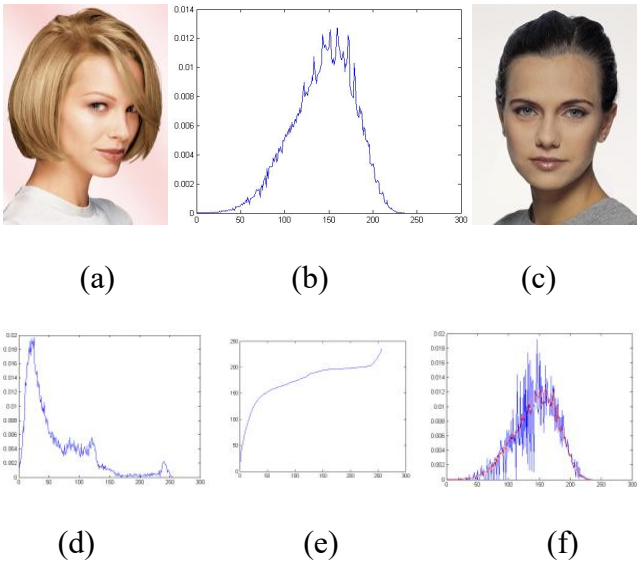

(a) (b) (c)

(d) (e) (f)

Figure 3. The model photo (a) (L'Oreal Paris Excellence 800) and its Y-histogram (b); The User photo (c) and its Y-histogram (d), YLUT function (e) and transformed Y-channel (y_t): user histogram (blue) superimposed with model histogram (red) (f).

To avoid heavy tails in the transformed distribution, the pixels, having $(U_t,\ V_t)$ values that violate inequality (8) are replaced with the model's average chromaticity $(\overline{U}_m,\overline{V}_m)$.

2.2. Hair Color Descriptor

The obtained Y histogram is split into no more than 20 clusters or slices (see Figure 2b) in such a way that each slice contains at least 5% of the distribution volume and has at least five bins. Since the human visual system (HVS) is susceptible to the blond colors, the brightest slice is recursively split into two slices if it contains more than 100 bins and more than 2.5% of the total distribution volume. Furthermore, the neighbor clusters having similar u^*v^* distributions by Hotelling criterion of multi-variance comparison with significance level 0.05, are merged (see Figure 4). This process is repeated until there exist two clusters, which have merged. The bounds of the final slices are saved at the training stage for each model and are applied to the user's hair at the color application stage (see Figure 4b). For each slice, the hole and petals are detected. The hole is the circular area in Figure 2b; it is defined as a cloud of pixels, having low saturation value (typically, $S \leq 5$) inside these holes hue values are unstable and cannot be appropriately detected. The pixels inside this area are transferred using

(3) and (4). The hue distribution for each slice is split into petals (see Figure 2b) using branch and bound clustering in the circular hue histogram. Every petal corresponds to a hair swatch; therefore, there are very few such petals for natural hair colors. Since the hue distribution is circular, a false zero is calculated and saved for every pie separately. The false zero is expected to be as far as possible from two nearest swatches. For the most natural hairs, it is around green color (148º). The circular shift is applied to the hue histogram. Thus, the false zero becomes a new origin, which prevents false cluster creation around the red color (0º). The process is accomplished with the clusters aggregation using the saturation distribution and the Student criterion about averages equivalence with significance level 0.05. If the final Hue-histogram has more than one petal, the histogram is quantized for 256 bins and saved; otherwise, parameters (M, Σ) (M, Σ) of the YSH normal distribution are kept for further applying to the user's hair.

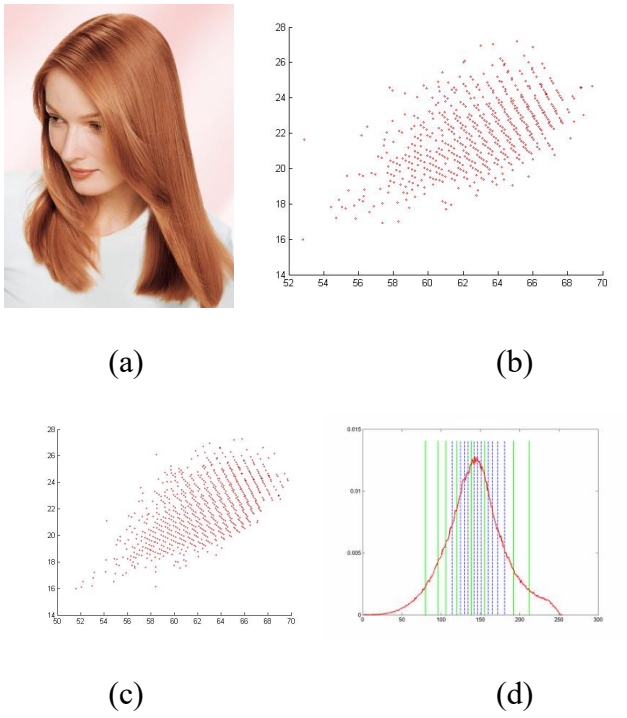

Figure 4. Slice merging for L'Oreal Paris Excellence 842 model (a), u^*, v^* distribution for slices 11 (b) and 12 (c), are merged using the Hotelling criterion with significance value 0.31. Original histogram, along with the final slices of intensity distribution (d).

2.3. Transferring of the Chromaticity Distribution in non-Gaussian Case

For each cone slice associated with a hair swatch, a Hue LUT (HLUT) is applying (Figure 5b) with the Gaussian-shaped Parzen window, having the standard deviation of 1.5/360°. This

process is the same 1D transform as YLUT (2) described above. The circularly of Hue histogram is carried out by using an optimal false zero angle H_0^M, calculated using the model Hue histogram. However, simple HLUT applying causes false-colors because of the high correlation between Y and H components, so the following correction is applied.

The average correction for every pixel can be obtained as a conditional expectation of the 2D Gaussian distribution:

$$m(H|Y) = \overline{H}_m + \rho_m(Y,H)\sigma_m^H\,(Y_t - \overline{Y}_m)/\sigma_m^Y, \qquad (9)$$

where $\overline{H}_m$ is the average model hue value for the slice $\rho_m(Y,H)$ is the model correlation ratio between Y and H components for the given slice, σ_m^H and σ_m^Y are the model standard deviations for Y and H components. In (9), Y_t is the user intensity value, transformed by YLUT and symbol $\overline{Y}_m$ denotes the average model slice intensity. This linear correction is processed using the cumulative hue distribution function (HCFD).

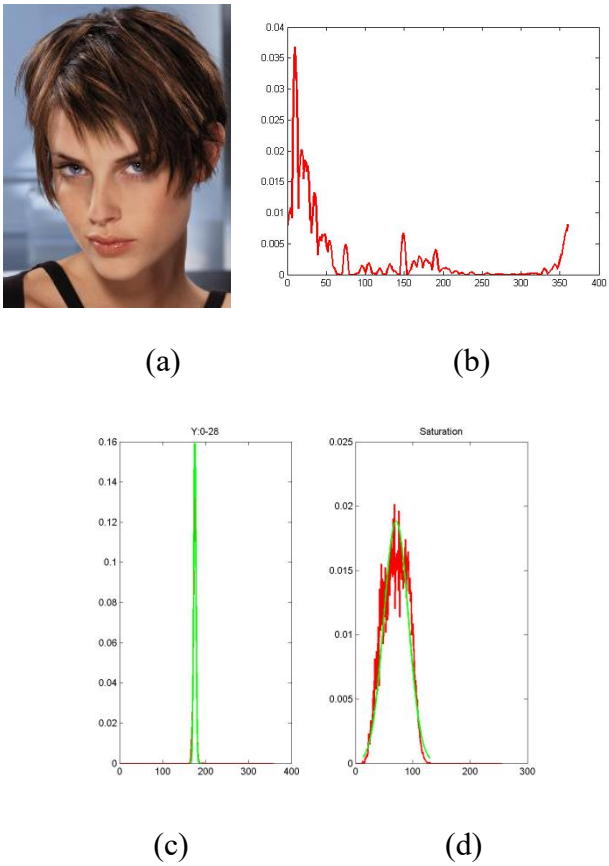

Figure 5. L'Oreal Paris Couleor Experte 500 model (a), Hue distribution for slice 3 (b), (HLUT example), and for slice 8 (c), (Gaussian example); saturation distribution for merged petals with the Student's significance 0.29 (d).

Let us suppose that $Q(h)\epsilon[0,1]$ denotes the HCFD of the hue value h. In this case, the corrected HCFD is:

$$P_h = Q(H_t) + Q(m(H|Y)) - Q(\overline{H}_m), \quad (10)$$

where notation H_t denotes the HLUT-transformed hue value. The average model hue value is $\overline{H}_m$ and the expectation $m(H|Y)$ is calculated by (9). The transform (10) is applied only to the pixels, having the corrected hue shifted towards the average:

$$(P_h - Q(\overline{H}_m))(Q(m(H|Y)) - Q(\overline{H}_m)) \leq 0. \quad (11)$$

The applying (10) under condition (11) allows preventing false coloring, showing up at the tails of the Hue distribution. Thus, the resulted hue for the given intensity is as follows:

$$\widetilde{H} = m(H|Y) + (F^{-1}(P_h) - m(H|Y))\sqrt{1 - \rho_m^2(Y,H)}, \quad (12)$$

where $F^{-1}(P_h)$ denotes a function, which is the inverse to HCFD. Eventually, the transformed hue values have to be clipped into the model bounds for the given slice $[H_{min},H_{max}]$.

The saturation is supposed to be always Gaussian, so for each slice, there is a conditional 2D Gaussian distribution S, H, depending on Y (see Figure 6). The conditional hue average is $m(H|Y)$ and the predicted conditional average of the saturation is written as:

$$m(S|Y) = \overline{S}_m + \rho_m(Y,S)\sigma_m^S\,(Y_t - \overline{Y}_m)/\sigma_m^Y, \quad (13)$$

where $\rho_m(Y,S)$ is the model correlation ratio between Y and H components for the given slice and the symbol σ_m^S denotes the model standard deviations for the saturation.

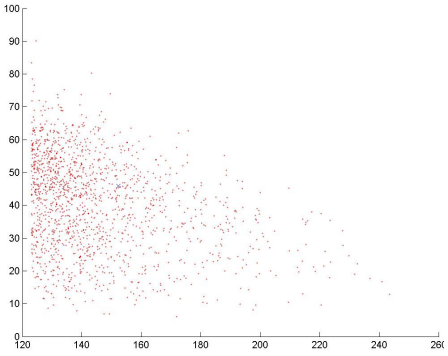

Figure 6. *Luminance (Y) – Saturation (S) scatter-plot for L'Oreal Paris Couleor Experte 535 mod el, slice 10.*

The conditional standard deviations are:

$$\sigma(S|Y) = \sigma_m^S \sqrt{1 - \rho_m^2(S,Y)}, \tag{14}$$

$$\sigma(H|Y) = \sigma_m^H \sqrt{1 - \rho_m^2(H,Y)}. \tag{15}$$

The conditional correlation ratio between them is:

$$\rho(S,H|Y) = \frac{\rho_m(S,H) - \rho_m(Y,H)\rho_m(Y,S)}{\sqrt{\left(1-\rho_m^2(Y,S)\right)\left(1-\rho_m^2(Y,H)\right)}}\ . \tag{16}$$

The resulted saturation is calculated, using expressions (13)-(15) as follows:

$$\tilde{S} = m(S|Y) + \sigma(S|Y)\,(s - \bar{S})/\sigma_S, \tag{17}$$

where s is the user's saturation at the transformed pixel. Value $\bar{S}$ is the average saturation over the user's slice distribution and σ_S denotes the standard deviation of the user's slice. Finally, the saturation (17) is clipped into the model bounds for the given slice $\tilde{S} \in [S_{min}, S_{max}]$.

2.4. Transferring of the Chromaticity Distribution in the Gaussian Case

In the Gaussian case (cf. Figure 5c), the model hue distribution for a slice consists of a small number of 2D Gaussian distributions $N_i(H, S)$ or petals of hue and saturation with relative volumes $a_i \in (0,1]$. In this case, the color transferring is based on a greedy solution of the assignment problem [6] that minimizes the sum of the absolute hue differences between the model and user images. This solution depends on the user's hue distribution. If the user's hue distribution cannot be decomposed into the separated Gaussian petals, (see Figure 5b, e.g.), then the matching is based on the circular shift of the user's hue distribution by the $H_0^M - H_0^U$ angle, where the angle H_0^U denotes the user's optimal false zero. The user to model petal assignment is processed as follows.

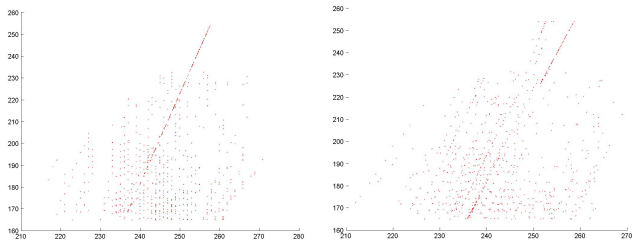

(a) (b)

Figure 7. Scatter plot of Y(Hue) distribution over the dominant petal of the brightest slice. User: see Figure 8a, model: L'Oreal Paris Couleor Experte 500 (see Figure 8b). The assignment, based on hue histogram color shift (a) and the dominant petal (b).

Let us denote as $cdf(H)$ the user's cumulative hue distribution for the given slice. The collection of $cdf(H)$ is starting from H_0^U in the counterclockwise direction. Let $A_n = \sum_{i=1}^{n} a_i$ is the sum of relative model's petal volumes, starting from H_0^M also in the counterclockwise direction. Obviously, $A_1 = 0$ and $A_N = 1$, where N is the total number of the model's petals in the given slice. Let H_n is the root of the equation $A_n = cfd(H_n)$, then the user's petal, assigned to the model's petal P_i consists of the user's pixels, having the hue values $H_n \le h < H_{n+1}$, where $n = 1,...,N$ and $H_1 = H_{N+1} = H_0^U$ because of the circularity of the hue distribution.

If the user's hue distribution can be decomposed into the petals (see Figure 5c), then a dominant petal, meaning the petal, having maximal relative volume, i.e., $arg\max_i a_i$, can be defined as for the user as for the model distribution. For adopted greedy matching, the user's dominant petal is assigned to the model's dominant petal. Let β_j, $j = 1,...,M$ are the relative volumes of the user's petals, then the user's petals $P_j, P_{j+1}...$ are assigned to the model's petal P_i to the right and the left to the dominant petal if $\beta_j + \beta_{j+1}... \le a_i$.

The transformed hue value in the user's petal is calculated as follows:

$$\widetilde{H} = \widetilde{H}_1 + \widetilde{H}_2 + m(H|Y), \tag{18}$$

where

$$\widetilde{H}_1 = \sigma(H|Y)(h - \overline{H})\sqrt{1-\rho^2(S,H|Y)}\big/\sigma_h \quad \text{and} \tag{19}$$

$$\widetilde{H}_2 = \sigma(H|Y)\rho(S,H|Y)\,(s-\overline{S})/\sigma_S. \tag{20}$$

Finally, the transformed hue the saturation values are clipped into the model's petal Hue-Saturation 2D-interval $[S_{min}, S_{max}] \times [H_{min}, H_{max}]$. Besides, to prevent false colors appearance condition (8) is applied to the transformed hue and saturation values as follows:

$$\frac{t_S^2+t_H^2-2t_S t_H \rho_m(S,H)}{1-\rho_m^2(S,H)} \leq -2ln(1-q), \qquad (21)$$

where $t_S = \left(\tilde{S}-\bar{S}_m\right)/\sigma_m^S$, $t_H = \left(\tilde{H}-\bar{H}_m\right)/\sigma_m^H$, $\bar{S}_m$ and $\bar{H}_m$ are the averages of the saturation and hue for the model's petal, values σ_m^S and σ_m^H denote are their standard deviations. In (21), the quantile $q = 0.95$. If a pair of transformed values $\left(\tilde{S},\tilde{H}\right)$ violates (21) it is replaced with the model's average $(\bar{S}_m,\bar{H}_m)$.

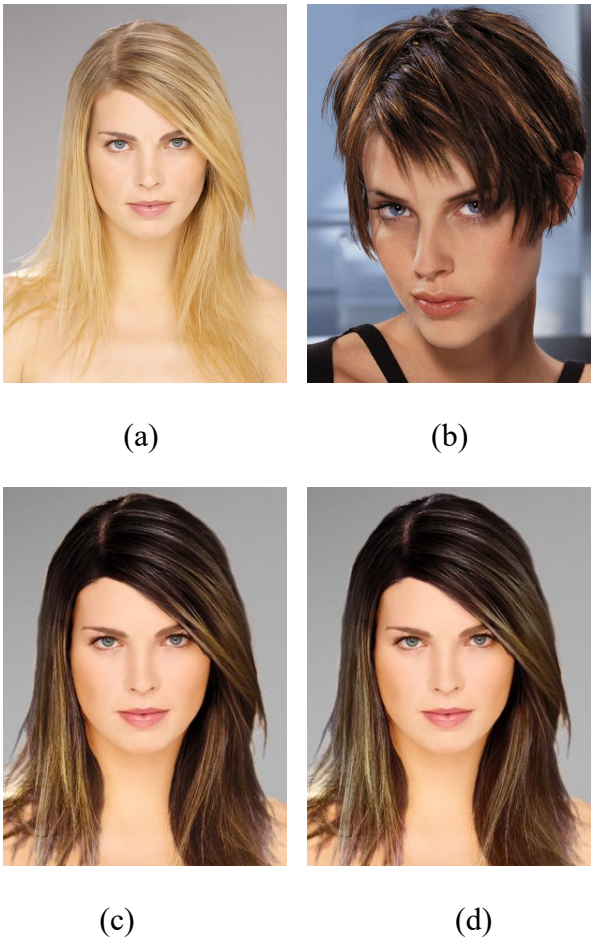

(a) (b)

(c) (d)

Figure 8. Hair colorization using Gaussian petals matching (c) and hue-histogram matching (d) of the user's image (a) with the L'Oreal Paris Couleor Experte 500 model (b).

To prevent false coloring, causing due to dependency on the intensity Y (see Figures 6, 7), let us introduce the relative intensity deviation from the given model average over the given slice:

$t_Y = (Y_t - \overline{Y}_m)/\sigma_m^Y$, where Y_t denotes the transformed intensity. Then the Mahalanobis distance to the center of the 3D-model's distribution is:

$$M_3 = \frac{2(K_{SH}+K_{SY}+K_{HY})+t_S R_{HY}+t_H R_{YS}+t_Y R_{SH}}{R_{HY}+R_{YS}+R_{SH}-2(1-\rho_m(H,Y)\rho_m(Y,S)\rho_m(S,H))}, \quad (22)$$

where

$$R_{HY} = \left(1-\rho_m^2(H,Y)\right), \quad (23)$$

$$R_{YS} = \left(1-\rho_m^2(Y,S)\right), \quad (24)$$

$$R_{SH} = \left(1-\rho_m^2(S,H)\right), \quad (25)$$

$$K_{SH} = \rho_m(H,Y)\rho_m(Y,S) - t_H t_S \rho_m(S,H), \quad (26)$$

$$K_{SY} = \rho_m(S,H)\rho_m(H,Y) - t_Y t_S \rho_m(S,Y), \quad (27)$$

$$K_{HY} = \rho_m(S,H)\rho_m(S,Y) - t_Y t_H \rho_m(H,Y). \quad (28)$$

(a) (b) (c) (d)

(e) (f) (g) (h)

Figure 9. Colorization with the L'Oreal Paris Excellence models: EX-100 (a), EX-416 (b), EX-654 (c), and EX-842 (d) of the original user's image from Figure 1 (a).User's colorized images: with EX-100 (e), EX-416 (f), EX-654 (f), and EX-842 (h).

The outliers are detected by using the inequality:

$$M_3\left(Y_t,\tilde{S},\tilde{H}\right) > a_3(q), \quad (29)$$

where $M_3\left(Y_t,\tilde{S},\tilde{H}\right)$ is calculated by (22)-(28) and $a_3(q)$ is a root of the equation:

$$errf\left(a_3/\sqrt{2}\right) - 2a_3 exp\left(-a_3^2/2\right)/\sqrt{2\pi} = q \qquad (30)$$

The transformed $\left(Y_t,\tilde{S},\tilde{H}\right)$ that satisfies (29), (30) with quantile $q = 0.95$ is replaced with the model's average $(\overline{S}_m,\overline{H}_m)$.

The results of the hue distribution transferring for the brightest intensity slice of the L'Oreal Paris Couleor Experte 500 model (see Figure 8b) to the user (see Figure 8a) are shown in Figure 7. Figure 7a displays the case of the non-Gaussian transferring, based on the hue-histogram. The distribution in the scatter plot in Figure 7a is concentrated close to the dominant petal. In the Gaussian case (Figure 7b), there are also other petals, alongside the dominant petal. Figure 8c depicts the results of the recolorization in the Gaussian case and Figure 8d for hue-histogram matching. The non-Gaussian case produces a bit less false colors and less vivid hair at the expense of the compression rate.

3. Experiments with Real Data

The proposed method was implemented in the EZface virtual colorist system and has been evaluated using EZface.com web site [16]. We use the set of 530 model images of different L'Oreal Paris hair color brands (see some examples in Figures 9a-9d) for quantitative evaluation. For the experiments, the model *RGB* images of 1200x1605 pixels were provided along with α hair mask. Figure 1c shows an example of a mask. Typically this mask is about 20 - 30% of the total model's hair area. The hair color model is created and saved separately for each model image, using this model image and the hair mask.

Table 2. Comparative study of hair colorization quality by different color transferring algorithms (PSNR in decibels)

Hair color number	Model description length (bytes)	Color transfer brush [10]	Tai et al. [13]	Xiang et al. [14]	The proposed method
200	2,974	26,8	32.0	31.2	33.0
210	2,874	27.8	30.8	31.9	38.0
300	2,413	30.7	38.8	39.3	40.9
316	2,744	21.8	26.0	26.7	27.9

400	2,744	28.9	36.9	37.0	40.2
415	1,571	25.3	32.8	33.5	37.7
426	1,859	26.1	36.9	36.8	41.4
500	565	25.8	31.6	31.4	31.7
565	1,738	24.0	30.2	30.2	36.4
600	888	26.0	36.1	34.6	37.9
643	1,153	25.9	37.3	37.3	46.5
645	997	24.9	34.0	34.0	40.5
656	763	26.1	38.0	38.0	45.2
700	1,197	26.8	39.7	39.6	41.4
713	1,903	25.8	39.1	39.4	44.0
724	697	26.5	36.9	36.9	47.2
810	837	26.2	40.5	40.8	40.9
832	653	25.5	34.0	34.0	39.7
834	960	23.8	30.9	30.9	35.3
930	969	31.8	32.3	28.2	34.4
Average	1,525	26.3	34.7	34.6	39.0

The user's image (see Figure 1a) is processed by the algorithm [9] for hair detection (see Figure 1b). Then, the hair color transfer is applied to the detected hair area, using the saved hair color models. At every user's hair pixel, the transformed color $\left(Y_t,\tilde{S},\tilde{H}\right)$ is converted into the RGB color space and as a result, we get pixel $\tilde{I} = (R_t,G_t,B_t)$. Eventually, this pixel is blended with the original RGB user's hair color pixel, providing the hair mask $\alpha(x,y)\epsilon[0,1]$. Therefore, the final image is:

$$I_F = \alpha\tilde{I} + (1-\alpha)I_0, \tag{31}$$

where I_0 is the original image and $\tilde{I}$ denotes the transformed image. The examples of the finally colorized user images are shown in Figure 9e-9h for the models, provided above in

Figure 9a-9d.

To evaluative quantitatively the quality of the hair colorization, let us colorize the model's hair. The first time the hair color distribution is created, using a small hair mask (cf. Figure 1c) and is kept for the next stage. The second time this hair color distribution is applied to the full model's hair mask (cf. Figure 1b). The resulted colorized hair is compared to the original model's hair, and the difference is measured. Thus, it is possible to compare the proposed method with other existing color transferring algorithms.

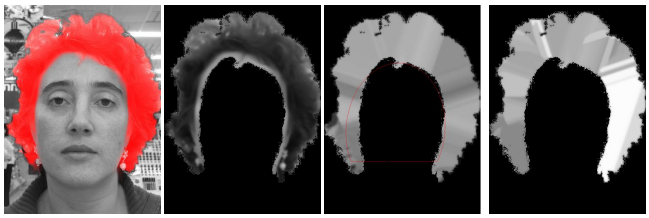

(a) (b) (c) (d)

Figure 10. Hair maximal intensity: Original user's image with hair mask (a), maximal intensity defined on the hair area (b), on the hair and open skin areas (c), and the hair, skin, and near background areas(32) (e).

The quality of the color transferring is compares using peak signal to noise ratio (PSNR) value, which is defined as follows:

$$PSNR = 10log\left(\frac{3S_M(256)^2}{\Sigma_{RGB}\Sigma_{Mask}\left(I_{ij}-I_{ij}^*\right)^2}\right), \qquad (32)$$

where S_M is the number of pixels in the hair mask $\alpha(x,y) > 0.1$, I_{ij} is original hair image and I_{ij}^* is finally transformed image (31).

The PSNR value (32) is more proffered in cosmetic applications than standard ΔE_{94} measure because of higher sensitivity to peak false-color errors, making simulation non-realistic [13], [14]. The quality of the color transferring is comparing using PSNR values (32), which are collected in Table 2 for different colorization techniques. There are 20 illustrative examples of the colors in Table 2, which are compared using four algorithms: Color transfer brush algorithm [10], EM-segmentation in $l\alpha\beta$ color space [13], GMM color transfer [14] and the proposed method. The first column (Hair Color Number) of the table denotes the number of L'Oreal Paris Excellence hair color, which typically looks like the image in Figure 9. This result is compared with the original model image, and the PSNR value is measured. Columns

3-5 of the table contain the PSNR values for different color transferring algorithm and the second column indicates the model description length in bytes. The last row in the table summarizes average values for the overall set of 530 model images.

4. Hair Relighting

The proposed hair colorization algorithm supposed the hair color reproduction of the model's hair in the user's photo exactly as far as possible. However, sometimes the illumination in the user image is too different from the standard light source in the model image. This difference causes the colorized hair looks unnatural over the user's face and its background. In this case, the user's colorized hair should be adjusted to the user image illumination.

(a) (b) (c)

Figure 11. Examples of automatic sclera detection in the user's (a, b) and the model's (c) images.

The visible reflected hair color $Y(C)$ can be modeled [5] as a product of the incident light L and the albedo of the colorized user's hair $a(C)$, i.e., $Y(C) = La(C)$. However, the light source in the user's image is unknown and should be estimated. Then, colorized hair should be changed to fit the estimated user photo illumination.

4.1. Intensity Relighting

The problem of unnatural hair intensity is shown up mainly over the blond hair. Therefore, only the maximal available light intensity of the hair should be estimated in the user image. The hair intensity map estimation is the maximum of three components:

$$L_{map} = max(L_{hair}, L_{face}, L_{bg}), \quad (32)$$

where L_{hair} is the intensity of the original user's hair, L_{face} is the intensity face skin, close to the user's hair area, and L_{bg} denotes the intensity of the background in the user's hair

vicinity.

The user's hair intensity map is Y component of the Yu^*v^* color space, calculated using hair map $\alpha(x,y) > T$ (see Figure 10a), where threshold $T \in [0.005, 0.01]$. The hair image is blurred with Gaussian filter $G(\sigma)$, where $\sigma = 0.015D$, where D is the intraocular distance. The Gaussian blur helps to diminish the effect of the uneven hair intensity distribution and create a homogeneous map. Finally,

$$L_{hair}(x,y) = (Y_u|\alpha(x,y) > T) * G(\sigma), \qquad (33)$$

where Y_u is the initial intensity of the user's hair and $*$ denotes the convolution operation. Figure 10b shows an example of (33) convolution.

The hair intensity map, based on facial region intensity, L_{face} in (32) is estimated using detected facial skin [9]. The open facial skin detection is a by-product of the automatic hair mask detection [9]. Figure 11 illustrates examples of the open facial skin along with other facial features detection for the users and the model images. Using this open skin, facial mask $\alpha(x,y)$, mouth and eyes location, the face is approximated with an ellipse, having the axis (a, b) [9]. The intensity of the open skin is propagated towards the hair mask, using recurrent dilation on the intensity component with radial dilation kernel, having the radius $R_f = min(a, b)/9$. Finally, this dilated hair image is blurred with Gaussian filter $G(\sigma)$, where σ is the same as for L_{hair} map. Figure 10c shows the result of the maximal intensity between L_{hair} and L_{face} i.e., $max(L_{hair}, L_{face})$.

(a) (b) (c) (d)

Figure 12. Examples of the luminance only hair relighting: Original image (a), intensity hair map (32) (b), Initial hair recoloring in EX-800 (c), Hair intensity correction for the map (b) (d)

The hair intensity map, based on background intensity close to the hair, L_{bg} in (32), is estimated using small hair vicinity outwards the user's face. This vicinity is empirically defined as $0.075D$, where D is the intraocular distance. The distance transform allows

delineating the vicinity region. A radial dilation kernel, having the radius R_{bg} = 4 pixels is used to fill the hair region with the background intensity. Figure 10d depicts an example of the final hair map (32).

The hair relighting is processed if the estimated map (32) is significantly darker than the blond hair color. As a reference for the blond hair, L'Oreal Paris Excellence 800 (EX-800) has been selected. Initially, the user's hair is colored in EX-800 (see Figure 12), then the average intensity over the hair mask is estimated as:

$$\mu_{800} = average(Y_t|\alpha(x,y) > T), \quad (34)$$

where Y_t denotes the transformed intensity in the user's hair. Using the average (34) the relative environmental darkness is calculated as:

$$\alpha_{env} = 100\frac{\sum_{\alpha(x,y)>T}(L_{map}(x,y)<\mu_{800})}{\sum \alpha(x,y)>T}\% \quad (35)$$

The relighting is applied if $\alpha_{env} > T_{env}$, where an empirical threshold T_{env} is selected as T_{env} = 8%. In this case, the average transformed hair intensity should be reduced by ΔK_{env}, where

$$\Delta K_{env} = med(Y_t|Y_t > L_{hair}) - med(L_{hair}|Y_t > L_{hair}), \quad (36)$$

where $med(.)$ denotes the median. Finally, the target hair intensity average after the relighting is $\mu_\gamma = \mu_{800} - \Delta K_{env}$.

The hair relighting is processed via gamma-correction of intensity channel $Y \in [0, 1]$:

$$Y_\gamma = \left(\frac{Y-Y_{min}}{1-Y_{min}}\right)^\gamma, \quad (37)$$

where the minimal intensity over transformed hair intensity $Y_{min} = min(Y_t)$. Parameter γ is constant per user's image and is calculated as the root of the equation:

$$\sum_{i=1}^{N} y_i^\gamma = Nm_\gamma, \quad (37)$$

where $y_i = (Y-Y_{min})/(1-Y_{min})$. Figure 12d displays an example of the hair relighting with $\gamma = 1.42$.

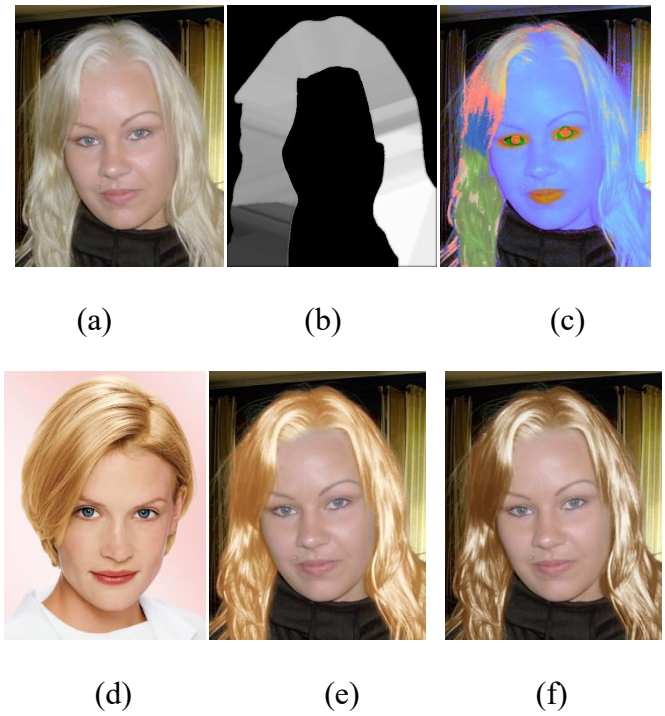

(a) (b) (c)

(d) (e) (f)

Figure 13. Examples of the hair relighting and white rebalancing: Original user's photo (a), hair illumination map (32) (b), facial features map (c), model's image of EX-930(d), initial hair recoloring(e), hair after relighting and white rebalancing (f).

4.2. White Rebalancing

When the light source of the captured user's photo significantly differs from the light source of the model's image, the colorized hair also gets a color cast. This cast causes the hair to look unnaturally different from the user's face. In this case, the hair appears with a reddish cast under a low color temperature light source and with a bluish cast under a high-temperature light source.

To define the color temperature of the light source, the white patch method of the white balancing [3], [11] is used. Typically, for a white patch, a bright white area of the image is used [5], [3]. For a human face, such a spot is eye sclera, which is detected as a by-product of automatic hair detection [9]. Figures 11 and 13c give some cases of eye sclera detection.

Only 30% of the top brightest pixels of the eye sclera are considered as a white patch to reduce the impact of the artifacts of the eye sclera detection. The average saturation of the white patch $\bar{S}_{70}$ is calculated separately for both eyes as follows:

$$\bar{S}_{70} = average(S(x,y)|Y(x,y) > Y_{70}), \qquad (38)$$

where Y_{70} is the root of the equation: $cdf(Y) = 0.7$, where Y is the intensity distribution over the eye sclera and $cdf(Y)$ is the cumulative distribution function of Y. If the saturation is significantly different between the two eyes, i.e.

$$\Delta S = \frac{|\bar{S}_{70}(Left) - \bar{S}_{70}(Right)|}{max(\bar{S}_{70}(Left),\ \bar{S}_{70}(Right))} > 0.3, \qquad (39)$$

where $\bar{S}_{70}(Left)$ is the saturation of the left eye and $\bar{S}_{70}(Right)$ of the right eye, then $\bar{S}_{70} = min(\bar{S}_{70}(Left),\ \bar{S}_{70}(Right))$. If the condition (39) is false, then calculation (38) is processed for the merged distribution of both eyes. If the average saturation is low, say $\bar{S}_{70} < 25$, it is supposed the hair color is already correct. Otherwise, the first iteration [3] is applied as: $U' = U + \Delta\bar{U}$, $V' = V + \Delta\bar{V}$, where (U, V) is transformed hair chromaticity in YUV color space, (U', V') is white rebalanced hair chromaticity and corrector $(\Delta\bar{U}, \Delta\bar{V})$ is define as follows: $\Delta\bar{U} = \bar{U}_{70} - U_{800}$ and $\Delta\bar{V} = \bar{V}_{70} - V_{800}$. The values $\bar{U}_{70}$ and $\bar{V}_{70}$ are calculated using (38) for the components (U, V) over the eyes sclera and the reference constants U_{800} = 0.043 and V_{800} = 0.015 are derived from the eye sclera of L'Oreal Paris Excellence 800 model image (see Figure 3a).

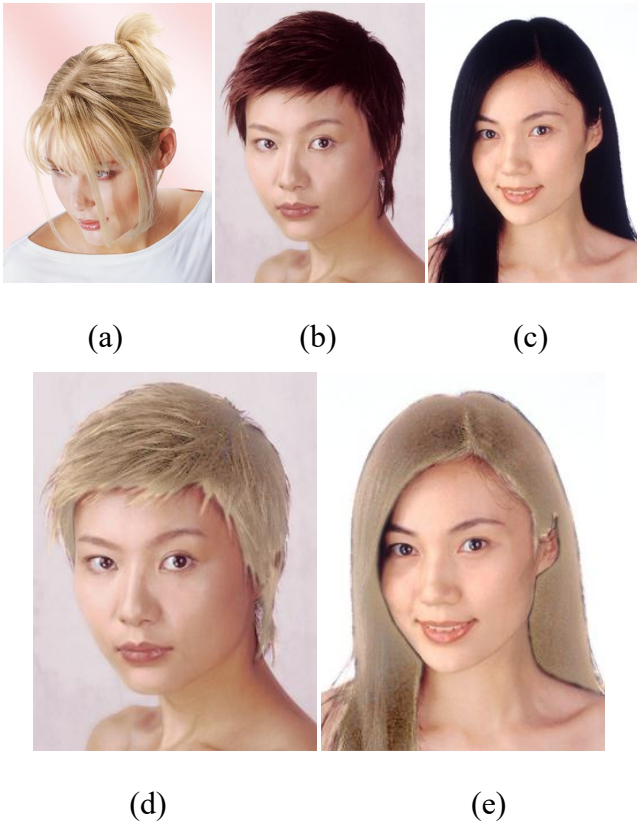

(a) (b) (c)

(d) (e)

Figure 14. Examples Chinese Girl Problem: Model's image of CE-910 (a), original users' image (b, c), colorized users' image (d, e).

An example of hair relighting, including white rebalancing, is provided in Figure 13 for the blond hair L'Oreal Paris Excellence 930 (EX-930).

5. Conclusion

In this paper, the hair colorization technique, based on the mixing of 3D Gaussian and non-Gaussian color transferring, has been proposed and evaluated for the virtual hair color modeling. Experiments, based on the results of EZface product exploitation [16], show that the proposed algorithm outperforms state-of-the-art techniques for the hair colorization for all types of hair colors (see table 2) and has reasonable model description length, suitable for transferring via the Internet. The proposed hair relighting, accomplished with white rebalancing, allows adjusting a standard hair model light source to the user's light source. The light source adjustment makes the user's colorized hair vivid and photorealistic. Numerical experiments with more than 20,0000 users' hair recolorization (see, e.g., figures 9, 12, 13) have been done for a variety of hair colors. These experiments show high colorization quality almost at just-noticeable distortion levels. Eventually, the proposed colorization produces a photorealistic effect.

A natural limitation of the method, derived from the requirement of the user's hair texture preserving, shows up when wide dynamic range blond hair, like EX-930 (Figure 13d) or CE-910 (Figure 14a), is transferred to the black hair users depicted in Figures 9a, 14b, 14c. In this case, which we call the Chinese Girl Problem (CGP), only a few different colors, corresponding to the number of the different user's hair swatches, are transferred to the colorized user's hair. Eventually, this causes a poster-effect that is illustrated in Figures 14d and 14e, which is resulted in the recolorization of users, shown in Figures 14b and 14c in Couleor Experte 910 color, given in Figure 14a.

References

[1] Badrinarayanan, V., A. Kendall, and Cipolla, R. (2016). SegNet: A Deep Convolutional Encoder-Decoder Architecture for Image Segmentation. arXiv:1511. 00561v3.

[2] G. R. Greenfield and D. H. House, "A palette-driven approach to image color transfer," in

Computational Aesthetics in Graphics, Visualization and Imaging, L. Neumann, M. Sbert., B. Gooch., and W. Purgathofer, Eds. Eurographics Association, Goslar, Germany, 2005, pp. 91-99.

[3] Hou, J.-y. , Chang, Y.-l. , Wang, J., and X.-x. Wei (2006). Robust Automatic White Balance Algorithm using Gray Color Points in Images. IEEE Trans. on Consumer Electronics, 52(2): 541-546.

[4] Huang, H.-Z., S.-H. Zhang, R. R. Martin, and S.-M. Hu (2014). Learning Natural Colors for Image Recoloring. Pacific Graphics, 33 (7): 299–308.

[5] Kawakami, R., Zhao H., Tan R. T., and K. Ikeutchi (2013). Camera Spectral Sensitivity and White Balance Estimation from Sky Image. International Journal of Computer Vision, 105: 187-205.

[6] Kuhn, H. W. (1957) The Hungarian method for the assignment problem. Naval Research Logistics Quarterly, 2: 83–97.

[7] Levin, A., Lischinski, D., and Y. Weiss (2008). A Closed-Form Solution to Natural Image Matting. IEEE Trans. Pattern Analysis and Machine Intelligence, 30(2): 228-242.

[8] Lin, S., Ritchie, D., Fisher, M., and P. Hanrahan (2013). Probabilistic color-by-numbers: suggestion pattern colorizations using factor graphs. ACM Trans. on Graphics, 32 (4): 37.1, 2, 6, 9.

[9] U. Lipowezky, O. Mamo, and A. Cohen, “Using integrated color and texture features for automatic hair detection,” Proc. 25th IEEE Convention Electrical and Electronic Engineers in Israel, pp. 51-55, December 2008.

[10] Q. Luan, F. Wen, and Y.-Q. Xu, “Color transfer brush,” Proc. 15th Pacific Conference on Computer Graphics and Applications, pp. 465-468, 2007.

[11] Provenzi, E., Gatto, C., Fierro, M., and A. Rizzi (2008) A Spatially Variant White Patch and Gray World Method for Color Image Enhancement Driven by Local Contrast. IEEE Trans. Pattern Analysis and Machine Intelligence, 30(10): 1757-70.

[12] Reinhard, E., M., Ashikhmin, B., Gooch, and P. Shirley (2001) Color transfer between images. IEEE Trans. Computer Graphics and Applications 21(5): 34-41.

[13] Y.-W. Tai, J. Jia, and C.-K. Tang, “Local color transfer via probabilistic segmentation by

expectation-maximization," Proc. IEEE Computer Society Conference on Computer Vision and Pattern Recognition, vol. 1, pp. 747-754, 2005.

[14] Y. Xiang, B. Zou, H. Wang, H. Li, and Z. Xie, "Multi-source color transfer for natural images," Proc. 15th IEEE International Conference on Image Processing, vol. 1, pp. 469-472, 2008.

[15] Yacoob, Y., and L.S. Davis (2006). Detection and Analysis of Hair. IEEE Trans. Pattern Analysis and Machine Intelligence, 28(6): 1164-69.

[16] [Online]. Available http://www.ezface.com: EZface Virtual Mirror, EZface Inc., 2008.

[17] [Online]. Available http://www.taaz.com: Taaz.com/Photometria Inc., May 2008.

[18] [Online]. Available http://www.photoshopessentials.com/photo-editing/hair-color/page-2.php: Change Hair Color in Photoshop, Photoshop Essentials.com, 2009.